HHS Public Access

Author manuscript

Ophthalmol Retina. Author manuscript; available in PMC 2020 December 01.

Published in final edited form as:

Ophthalmol Retina. 2019 December ; 3(12): 1035–1044. doi:10.1016/j.oret.2019.07.016.

Outer Retinal Thickness and Fundus Autofluorescence in Geographic Atrophy

Diane L. Wang, MD[1], **Julia Agee, MD**[1], **Marco Mazzola, MD**[2], **Riccardo Sacconi, MD**[3], **Giuseppe Querques, MD, PhD**[3], **Alan D. Weinberg, MS**[4], **R Theodore Smith, MD, PhD**[4]

[1]New York University School of Medicine, New York, NY

[2]Ophthalmology Clinic, Department of Medicine and Surgery, University of Insubria Varese-Como

[3]University Vita-Salute, Milan, Italy

[4]Ophthalmology, Mount Sinai School of Medicine, New York, NY

Abstract

Purpose: Most studies of fundus autofluorescence (FAF) in geographic trophy (GA) have been non-quantitative, with inadequate registration of other image modalities. Furthermore, as pointed out in the recent Consensus Definition for Atrophy Associated with Age-Related Macular Degeneration (CAM) on optical coherence tomography (OCT), it is still unclear whether definitely decreased FAF (DDAF) would be correlated exclusively with a single category of OCT-defined atrophy. We sought to determine how FAF intensity in eyes with GA correlates with structural changes of the outer retina and choroid as seen on co-registered spectral domain OCT (SD-OCT) images.

Design: Retrospective cross-sectional.

Subjects: 20 eyes of 11 patients with GA secondary to non-neovascular age-related macular degeneration (AMD).

Methods: SD-OCT and FAF images for each eye were co-registered with MATLAB. On B-scans, the choroid, retinal pigment epithelium (RPE), photoreceptor (PR) layer, and outer nuclear layer (ONL) were segmented. Regions-of-interest (ROIs) including all atrophic and border regions were selected manually on the FAF scans. ROIs were subdivided into quartiles of FAF level to correlate with retinal thickness measurements taken along the B-scans. Mean choroid, RPE, PR and ONL thicknesses were compared across quartiles using an Analysis of Variance (ANOVA) factorial design testing for interaction effects, adjusted for repeated measures (on both eyes) with a within-subjects factor.

Results: 17 eyes of 10 patients were selected for analysis. The mean choroidal thicknesses were not significantly different across FAF quartiles, but he overall differences in mean RPE, PR layer

Address for reprints: 310 E 14th St NYC, NY10003.

Conflict of Interest: No conflicting relationship exists for any author.

and ONL thicknesses across quartiles were statistically significant (ANOVA, $p<0.001$, $p<0.001$ and $p=0.015$, respectively). Post hoc analysis demonstrated significant differences in thickness between quartiles 1, 2 and 3 for the RPE and PR layers (Tukey, $p<0.01$ in each case). FAF quartiles within GA did not correlate exclusively with single categories of CAM-defined atrophy

Conclusions: Not only RPE, but also PR layer thickness on SD-OCT varies significantly with FAF levels in GA. This suggests that while the RPE cells are losing thickness and function, evidenced by decreased FAF from fluorophores, delicate PR cells also physically succumb early in the disease process. These relationships should be pursued as a possibly better-detailed mechanism in GA.

INTRODUCTION

Geographic atrophy (GA) is the advanced stage of dry or non-neovascular age-related macular degeneration (AMD) and is characterized by the loss of photoreceptors, retinal pigment epithelium, and choriocapillaris.[1] It affects approximately 5 million people worldwide, usually occurring bilaterally and can lead to irreversible vision loss.[2] While intraocular injections are used to treat the wet or neovascular form of advanced AMD, there are currently no available treatments available to reverse, prevent, or reduce the rate of progression of GA. Furthermore, the pathogenesis of GA is still poorly understood despite findings that show it occurs 4 times more frequently than neovascular AMD in adults aged 85 years and older.[1]

Various imaging methods and histopathologic studies have characterized GA as a progressive loss of photoreceptors, retinal pigment epithelium (RPE), and choriocapillaris perfusion. On color fundus photography (CFP), there is increased visibility of underlying choroidal vessels and sharply demarcated areas of RPE hypopigmentation.[3] On fundus autofluorescence (FAF), there is hypoautofluorescence in areas of GA due to loss of lipofuscin resulting from RPE cell death. FAF imaging of atrophic regions are highly correlated with regions seen on CFP, but with better clarity, contrast, and reproducibility, and thus has become the primary method to detect, monitor, and quantify atrophic lesions.[4,5] Optical coherence tomography (OCT) imaging allows cross-sectional evaluation of the retina, and of note, *complete* morphologic absence of the RPE layer by spectral domain OCT (SD-OCT) is significantly smaller than the GA size in FAF determined by definitely reduced AF (DDAF)[6]. SD-OCT is also the basis for the new, staged Consensus Definition for Atrophy Associated with Age-Related Macular Degeneration.[5] Thus there is complete atrophy of the RPE and outer retina (cRORA), with complete loss of these layers, and incomplete RPE and outer retinal atrophy (iRORA), where some hypertransmission is evident but is discontinuous; the RPE band is present but irregular or interrupted. An interrupted external limiting membrane (ELM) and ellipsoid zone (EZ) evidence photoreceptor degeneration. In areas where the RPE is largely intact, there may be incomplete outer retinal atrophy (iORA) with residual photoreceptors or complete outer retinal atrophy (cORA) with complete loss of photoreceptors. We will use these terms where applicable, and also continue to use the general term GA, whose regions seen on SD-OCT show loss of outer retinal layers, increase in choroidal reflectivity below Bruch's membrane due to RPE loss, descent of the external limiting membrane (ELM) to Bruch’s membrane

(BrM), and loss of the choriocapillaris layer.[7,8] Histopathologic studies have shown similar findings – decreased BrM thickness, scrolling of the degenerating photoreceptors by Muller cells (ELM descent), and decreased choriocapillaris density.[8,9] Indeed, Curcio et al. calls the choriocapillaris the "photoreceptor supporting system", and its degeneration is seen between healthy and atrophic regions in eyes with GA, when the GA border is defined as the point of ELM descent.[9]

Many studies, both longitudinal and cross-sectional, have been done to characterize GA using multiple imaging modalities, and clarify its pathogenesis. Smith et al. found that GA progressed more significantly in areas with subretinal drusenoid deposits (SDD), also known as reticular pseudodrusen, suggesting that there may be a common underlying pathophysiology between SDD and GA, such as choroidal perfusion defects.[10]Another study pointed to the high correlation between presence of SDD and the presence of GA, suggesting that the SDD are an early manifestation of the process leading to GA.[11]Wu et al. described features of "nascent" GA as collapse of the IPL and ONL in areas initially occupied by drusen on SD-OCT, along with both hyperAF and hypoAF changes on FAF. [12,13]Studies investigating the shape of GA lesions found that the parameters of lesion circularity, diameter, area, and perimeter can predict disease progression rates.[14,15]Cousins et al showed that increased total autofluorescence in GA borders can indicate faster-progressing total (not local) atrophy.[16] On correlation with OCT, the reason for this perilesional hyperautofluorescence seems to be outer retinal disruption (with associated loss of blocking photopigment) and increase in RPE-basal lamina thickness. [17] On histopathology the mechanism likewise appears to be anterior migration and heaping up of RPE at the GA margin. [7,18]

What has not been investigated until very recently is that even *within* GA lesions, the levels of autofluorescence are not uniformly low, but can vary regionally between lobules and focally within lobules, suggesting non-uniformity of the GA process.[19] To examine these phenomena in detail, we have made use of the high resolution OCT and FAF images from the well-characterized cohort of GA subjects recently published by Sacconi et al. [20] Those authors found a reduction in choriocapillaris density on OCT angiography (OCTA) in the GA transition zones with non-atrophic RPE, suggesting that choriocapillaris damage may precede RPE damage.[20] For this study we focus on the relationships between the structural OCT data and varying FAF levels within and around GA lobules, to determine the structural correlates of FAF. In this regard, we will pay primary attention to the thickness of key outer retinal layers, and also will consider the consensus-defined stages of atrophy associated with FAF levels, in the transition zones, in "preserved" regions of relative hyperautofluorescence in and around GA lobules, and in the GA lesions themselves. To accomplish this, we will also implement a robust comparison between OCT and FAF images, overlaying the two images using a precise co-registration methodology. This is necessary to compare small regions within, and narrow margins around, the GA lobules themselves.

Another important limitation of most previous studies is that FAF reading was qualitative only, thus not allowing precise, objective, and repeatable evaluation. In our study, on the other hand, the FAF grayscale intensities within the region of interest (ROI) were automatically obtained at each pixel and divided into quartiles. To the best of our

knowledge, we are the first to introduce this semi-quantitative approach, which we believe can be usefully replicated in future studies. We hypothesized that there would be significant differences in the measured thickness on SD-OCT in one or more of the outer retinal layers (choroid, RPE, photoreceptor layer (PR), and outer nuclear layer (ONL) across regions of differing autofluorescence quartiles measured on FAF imaging. We also endeavored to determine what relationships might obtain between stages of atrophy and FAF levels.

METHODS

Subjects

20 eyes of 11 patients with GA secondary to non-neovascular dry age-related macular degeneration were selected for this study. All patients had presented at the Medical Retina and Imaging Unit of the Department of Ophthalmology, University Vita-Salute, Ospedale San Raffaele in Milan between August 2016 and February 2017. This retrospective study adhered to the tenets of the declaration of Helsinki and was approved by the ethics committee of San Raffaele Hospital. Written and informed consent was obtained from all patients. Inclusion criteria included diagnosis of dry AMD with GA, with GA defined as any sharply demarcated unifocal or multifocal area of absence of the RPE larger than 175 mm in diameter.[20]Eyes with poor quality SD-OCT scans were excluded.

All patients underwent a complete ophthalmologic examination, including best-corrected visual acuity using Early Treatment Diabetic Retinopathy Study (ETDRS) charts, slit-lamp biomicroscopy, tonometry, indirect fundus ophthalmoscopy, near infrared reflectance (NIR-R), FAF, SD-OCT, and SD-OCT angiography scans of the macula. NIR-R, FAF, and SD-OCT, were performed with the Spectralis confocal scanning laster ophthalmoscope (cSLO) (Heidelberg Engineering, Heidelberg, Germany). To achieve good visualization of the choroid, enhanced depth imaging-OCT (EDI-OCT) was used in all acquisitions. All NIR-R, FAF and SD-OCT scans were reviewed for the presence or absence of drusen and SDD.

SD-OCT analysis

Volumetric SD-OCT images for each eye were acquired covering 30° × 25° of the retina centered on the fovea, composed of 241 B-scans. Each of the B-scans were acquired in register to a NIR-R scan acquired by the Spectralis simultaneously. The 1st B-scan, then every tenth B-scan, was segmented pointwise manually (approximately 25 points selected per scan boundary). The (x, y) coordinates of each point in the boundaries of the choroid, RPE, PR layer, and ONL were stored in a MATLAB dataset (MathWorks Inc., Natick, MA, USA). These segmentations were then smoothed using cubic interpolation to give finer segmentations at the original scale (Fig. 1). Thicknesses were calculated by subtracting the y-values of the segmentation lines at each point at 496 evenly spaced points across each B-scan. Automation was not used in the segmentations.

FAF analysis

All eyes had FAF images taken on the same day as the SD-OCT. The grayscale FAF images were co-registered with their respective NIR-R images. Using a Matlab program, 6 points (typically at intersections of blood vessels) were manually selected on the FAF image, and

the same 6 points were selected on the IR image. Then, the program co-registered the FAF to the NIR-R image by rotating, scaling and non-linear stretching as needed, thus allowing both images to have the same coordinate system. The quality of co-registration was carefully checked by using Photoshop to overlay the co-registered images (Fig. 2).

GA Analysis

Regions of interest (ROI) containing GA, as seen on co-registered FAF images, were manually selected using a MATLAB program by an experienced grader. ROIs were selected to encompass all atrophic lobules and at least 500-micron margins that included bordering "normal" regions, for examining the transition zones between normal-appearing retina and atrophic regions. The ROIs were superimposed onto the co-registered NIR and FAF images for each eye (Fig. 3). NIR-R was used to determine foveal involvement in cases where low AF levels could be attributed either to GA or to macular pigment. In the latter case, the involved area was excluded.

Within the ROI for each eye, the AF grayscale intensities at each pixel were obtained. To minimize artifact from blood vessels and other outliers, the highest and lowest 2.5% of gray level values were excluded. The remaining values were divided into quartiles, and each quartile value was color coded. (Fig. 3). The first quartile corresponded with the lowest gray levels and the fourth quartile with the highest. At each pixel along each registered B-scan within an ROI, the FAF quartile values were extracted and stored along with the previously stored thicknesses of choroid, RPE, PR, and ONL at the corresponding locations. For every FAF quartile value, and for each retinal layer, the mean thickness across all ROIs of all points in that quartile and in that layer was calculated. Using FAF quartile as the independent variable, the differences in thicknesses across quartiles for each of the 4 retinal layers were compared using Analysis of Variance (ANOVA) factorial designs, whereby two or more experimental factors are studied and analyzed simultaneously, with repeated measures with a within-subjects factor. Specifically, both a three factor experiment with repeated measures on all factors (Retinal Layer, Eye and Quartile) and a two factor experiment with repeated measures on two factors (Retinal Layer and Eye) were utilized. These models also tested for interaction effects. Formally, interaction between two factors means the effect of one factor is not constant, but depends on the level of the other factor. All data was analyzed using SAS system software, Version 9.4 (SAS Institute Inc., Cary, NC).

RESULTS

Demographics

A total of 17 eyes of 10 patients were analyzed. 3 eyes of 2 patients of the original set were excluded due to poor scan quality. The mean age of the analyzed patients was 77.3 ± 4.9 years old. Of the total 10 patients, 7 were female, 8 had hypertension, 6 had hypercholesterolemia, and 2 had coronary artery disease. All eyes had multiple SDD.

GA Characteristics

The mean area and standard deviation of the ROIs encompassing GA in the 17 eyes was 5.13±2.79mm^2. The smallest ROI was 1.96mm^2 and the largest ROI was 10.68mm^2. In all 17 eyes, GA involvement included the fovea, in whole or in part.

Retinal Layer Thicknesses and FAF Quartiles

The differences in mean RPE, PR and ONL retinal layer thicknesses across FAF quartiles from all ROIs of the 17 eyes were statistically significant overall by ANOVA with repeated measures with a within-subjects factor (Table 1). The mean RPE thicknesses were 21.95, 27.91 32.46 and 34.02 microns in the 1st , 2nd, 3rd and 4th quartiles ($p<0.001$). The mean PR thicknesses were 11.63, 20.87 , 29.22 and 31.84 microns in the 1st , 2nd, 3rd and 4th quartiles ($p<0.001$). The mean ONL thicknesses were 37.2, 43.8, 48.6 and 47.8 microns in the 1st , 2nd, 3rd and 4th quartiles ($p= 0.015$). By the Tukey multiple comparison post hoc analysis test (Fig. 4), we found that thicknesses in the RPE and PR quartiles were significantly different between all pairs of quartiles in each group ($p<0.01$) except for between the 3rd and 4th quartiles. No post hoc significant differences were found between ONL quartile thicknesses.

SD-OCT defined stages of atrophy and FAF Quartiles

SD-OCT B-scans passing through GA lobules, represented by areas of hypoautofluorescence on FAF, and surrounding areas demonstrated a variety of characteristic pathologies in addition to the overall thinning of retinal layers just noted. In particular, the consensus definitions of stages of atrophy can be evaluated in the regions defined by FAF levels. Thus, GA lobules demonstrated ELM descent to the RPE at their borders and increased choroidal reflectivity, as well as RPE/PR layer thinning (Fig. 5 , I and II).

Between, in, and around the atrophic lobules, there are discrete areas of “preserved” autofluorescence. For example, preserved FAF at the edge of a GA lobule may correspond to an area of heaped up RPE (Fig. 5 , III) as described by Curcio et al. [18] These spots fall in the 2nd, 3rd or 4th quartile on the FAF quartile maps and are often found either within (as in Fig. 5, I and II) or immediately surrounding (as in Fig. 5, III) the larger lobules, which are typically in the 1st quartile. In these preserved regions, corresponding SD-OCT scans typically revealed marked disruption of the RPE. In Fig. 5, III , an “island” of preservation seen on FAF localized to a region on SD-OCT demonstrating hyperreflective material impinging as far as the inner retina. This is an illustration of activated RPE cells migrating anteriorly, seen histopathologically in prior studies as a precursor to atrophy.[21,22]

Multiple small hypoautofluorescent lesions characteristic of SDD were frequently seen on FAF in the regions surrounding GA lobules. Correlation with B-scans revealed disruption and ragged thickening of the RPE, as well as the presence of SDD. This was particularly evident in the aforementioned spots of higher FAF quartiles that are seen within lobules of GA, and in the transition zones between atrophic lobules and preserved retina on FAF (Fig. 5, IV).

DISCUSSION

The purpose of our study was to determine how fundus autofluorescence (FAF) intensities correlate with structural changes of the outer retina and choroid in eyes with GA, as seen on co-registered spectral domain optical coherence tomography (SD-OCT) images. Although many studies have been done to characterize GA on multiple imaging modalities, most had certain limitations that we have tried to overcome.

First, most of the previous studies have concentrated on the changes in the transition zone, with the atrophic lobules treated as end-stage, uniform features. In fact, FAF shows clearly that GA lobules are hardly uniform, which is explicitly recognized herein. Thus, we analyzed the atrophic lobules and the transition zones around them as a single unit in each eye to search for structural changes in the outer retinal layers and choroid that correlated with these variable autofluorescence intensities. A second important limitation of most previous studies is that FAF reading was qualitative only, thus not allowing precise, objective, and repeatable evaluation of FAF levels. In our study on the other hand, the FAF grayscale intensities within the ROI were automatically obtained at each pixel and divided into quartiles. To the best of our knowledge, we are the first to introduce this semi-quantitative approach, which we believe can be usefully replicated in future studies.

More recently, the histopathological border of GA has been defined as the point of ELM descent to BrM, which delimits an area of marked gliosis and near-total photoreceptor depletion. Degeneration of supporting tissues such as RPE and CC across this boundary is gradual, and precisely described. [23] The functional changes to the rod and cone systems in the junctional zone have also been recently described in detail with patient tailored microperimetry, showing greater loss of rod function in zones closer to the GA border.[24]

Third, to take full advantage of a high resolution, multimodal approach, care must be taken in the co-registration of the different image modalities. For example, SD-OCT images are usually taken simultaneously and in registration with NIR-R images on the Spectralis by the eye-tracking feature, and point-to-point correlation can then be made *visually* with the Heidelberg software. Further, this also allowed us to construct a common mathematical coordinate system for B-scans with the NIR-R image in which to put *data* for analysis such as layer thicknesses from the SD-OCT B-scans. However, in our study and most others, the FAF data was acquired separately and hence was *not* automatically in registration with the SD-OCT B scans, thus limiting precise interpretation. An exception has been work from the Bonn group, who studied the margin of GA in great detail with co-acquired (accordingly co-registered) FAF and Heidelberg OCT B-scans [25] Our solution was to provide an exact point-by-point registration of the FAF images to the NIR-R images with Matlab software. This in turn registered the SD-OCT scans to the FAF scans in the common coordinate system now shared by all 3 modalities, allowing precise correlation of B-scan data with FAF quartile levels. Such precision is necessary to study multiple, varied pathologies that change at a small scale, especially within the transition zones. Likewise, in a study where careful co registration was applied, the area of atrophy measured by FAF was larger than any area graded by SD-OCT[26], emphasizing the care needed in comparing multiple modalities. The recently published Consensus Definition for Atrophy Associated with Age-Related Macular

Degeneration on OCT[5] has also stated that it remains unclear at the moment whether severely reduced FAF would be correlated exclusively with a single category of OCT-defined atrophy or if certain variations might be present. In our study, we provided an exact point-by-point correlation of these 2 imaging methods to help answer this question.

The results of this study reveal that not only the RPE, but also PR layer thickness decrease significantly in regions within and around GA as their corresponding fundus autofluorescence levels decrease. This may suggest that though the RPE is losing function, its thickness is preserved initially while the PRs lose thickness more quickly. Qualitatively, we also found that many cross sections through islands of preserved autofluorescence within GA lobules showed loss of PR thickness even when RPE was still present. This is in agreement with a study by Bearelly et al., who showed that PR loss occurs outside GA margins when GA is characterized by an abrupt transition from hyperreflectivity to hyporeflectivity in the choroid.[27] Indeed, the question of whether RPE or PR loss occurs first in the disease process is one that has been investigated in multiple prior studies. On histology, Sarks et al. described the area of atrophy as “persisting” photoreceptors atop a cluster of degenerating RPE, but in some areas the photoreceptors were completely gone,[8] also suggesting that PRs may actually be quicker to deteriorate in GA.

The small, preserved regions of higher FAF quartiles that were within and around the low FAF quartile lobules corresponded to RPE dysmorphia and thickening, PR loss, and normal to slightly increased choroidal transmission on SD-OCT, that is, features of incomplete RPE and outer retinal atrophy (iRORA). In addition, the ELM seemed to have particularly disintegrated in such junctional zones, indicating PR loss.[28] iRORA is thought to lead to complete RPE and outer retinal atrophy (cRORA) as the disease progresses.[5,13] Regions in the lower first and second quartiles of AF intensity demonstrated PR loss, with or without remaining RPE, i.e., with iRORA or cRORA in SD-OCT, Higher FAF quartiles could also show: intact RPE with residual PRs, that is, incomplete outer retinal atrophy (iORA), : or intact RPE and complete loss of PRs, that is, complete outer retinal atrophy (cORA) (Fig 5, III, D). Further studies are needed to approach the comparison from the SD-OCT side and clarify the sequence of events by characterizing FAF changes at different stages of atrophy on OCT.

Regarding the other studied layers, we found that overall the ONL thickness was positively correlated to FAF levels whereas the choroidal thickness was not. This is consistent with prior studies, which have shown that the ONL layer is thinner in regions where SDD are present,[29] and that in eyes with GA, the ONL showed a clear consistent trend for increasing cell counts with increasing RPE preservation.[30] Further, SDD may be a precursor to RPE loss and atrophy, leading to the cascade of events that results in atrophic AMD. In a study by Xu et al., it was observed that RMD is nearly universally present with multilobular GA in AMD, and lobules frequently develop in areas of RMD, suggesting a single underlying disease process.[10]

This study has several limitations. Firstly, our sample size (in subjects) is relatively small. However, many regions were examined, and nearly 500 measurements were taken from each B scan of layer thickness. In addition, statistical correction was made for measurements

from both eyes of a given subject. Another limitation is that FAF was performed with standard cSLO, and not with quantitative FAF (qAF) instrumentation, in which the AF image is calibrated to an embedded reference of known fluorescence efficiency.[31] qAF would have provided a better metric had it been available. The ranking of AF values in any given eye would not change, but better comparisons between eyes would have been facilitated. Thus, conclusions would have more general significance. The post-hoc analyses of the third and the fourth quartiles found that thicknesses were not significantly different among RPE and PR beween these groups (Figure 4). Thus, the value of these groups appears limited. This could in part be due to the natural distribution of the higher AF levels superiorly[32], resulting in the fourth quartiles tending to reside in healthier tissue further from the GA. Likewise, because AF is naturally lower inferiorly, these areas may be shifted towards the lower quartiles, and then may contribute increased RPE/ONL/PR thickness to the lower quartile groups. The effect on the results, however, would be only to blunt, rather than enhance, the thickness differences between quartiles, so would not detract from their validity. Furthermore, there can be actual uneven illumination (Fig 5, II), contributing to similar errors. OCT segmentation of complex pathology, manually or automatically, is difficult, and may not even be amenable to a provably correct solution in some cases. Our approach, a hybrid of manual point selection and computer interpolation, provided smooth segmentations that on review looked equivalent to a complete manual segmentation, the gold standard, but doubtless contained numerous errors. In the absence of detectable systematic bias, most errors should be small and random, and largely cancel at the level of noise.

Normative data, always of interest in measuring the deviation of a pathological state from the (age-matched) normal, was not considered, which could be considered a limitation. However, in the case at hand, the question is not *whether* loss of tissue and thinning of outer retinal layers occurs in GA, a given, but rather, can the a*mount* of outer retinal tissue loss in the complex pathology of GA be correlated with FAF, a single, critical and independent *en face* measurement, which was answered in the affirmative. Likewise, even though there are complex reasons for increased and decreased FAF, at least *some* of this variability could be correlated with other measurable structures with reasonable interpretation.

The special properties of the fovea offer challenges to such a study: blocking of FAF by macular pigment (MP) and a particularly thick ONL. NIR-R was used to determine foveal involvement in cases where low AF levels could be attributed either to GA or to macular pigment. In the latter case, the involved area was excluded. For cases in which the fovea was involved with GA, the AF quartile values were always low, 1 or at most 2, and often beneath the 2.5%-tile cutoff for data exclusion. Thus, any greater ONL thickness in the fovea was always assigned to a lower AF quartile, and hence, could have only *blunted* the association between ONL thickness and AF quartile rather than biasing the result.

The major strength of this study is the novel combination and detailed joint analysis of FAF and SD-OCT images in registration to probe FAF/structure relationships in regions of interest in and around the lesions of GA. In particular, the semi-quantitative assessment of the FAF signal in quartiles instead of a binary (atrophic, non-atrophic) classification permitted a more detailed yet unbiased sampling method by which to extract regions for

correlation with structural data. The structural data could then be analyzed together across these 2-D planar regions instead of in single B-scans.

In summary, there are many reasons for increased and decreased FAF. Some we know, and some we may not. Therefore, the purpose of the study was to assess, amongst this complexity, in these eyes, whether at least *some* of this variability could be correlated with other measurable structural components, e.g., width of retinal layers on SD-OCT. So to this extent we were successful, and other contributors to FAF variability remain to be tested. In particular, the variability of the AF signal is no respecter of the GA boundaries, and that despite this apparent mismatch between AF levels and the *accepted* definition(s) of GA, there *is* an anatomic correspondence between AF levels and well-defined, layered structures of retinal anatomy (RPE and PRs) that are precisely recognized on SD-OCT independent of specific disease lesions or definitions. Likewise, within the GA lesions themselves, which are defined variously in the literature, there is again variability of the AF signal, for which the retinal layers provide an anatomic correlation. Of course, further subdivision of the ROIs into only GA and/or only transition zone could yield further interesting informations of greater granularity, and should be taken up in further research.

In conclusion, from a disease mechanism point of view, our results suggest that while the RPE cells are losing thickness and function, as evidenced by decreased FAF from RPE fluorophores, delicate PR cells that depend on the RPE are also physically succumbing early in the disease process, as evidenced by PR layer thinning. These relationships should be pursued as a possibly better detailed mechanism in geographic atrophy.

Acknowledgments

Financial Support: NIH/NEI R01 EY015520 (RTS)

References:

1. Klein R, Klein BE, Knudtson MD, Meuer SM, Swift M, Gangnon RE. Fifteen-year cumulative incidence of age-related macular degeneration: the Beaver Dam Eye Study. Ophthalmology. 2007;114(2):253–262. [PubMed: 17270675]
2. Wong W, Su X, Li X, et al. Global prevalence of age-related macular degeneration and disease burden projection for 2020 and 2040: a systematic review and meta-analysis. Lancet Glob Health. 2014;2:e106–116. [PubMed: 25104651]
3. Fleckenstein M, Mitchell P, Freund KB, et al. The Progression of Geographic Atrophy Secondary to Age-Related Macular Degeneration. Ophthalmology. 2018;125(3):369–390. [PubMed: 29110945]
4. Valckenberg SS, Sadda S, Staurenghl G, Chew EY, Fleckenstein M, Holz FG. "Geographic Atrophy": semantic considerations and literature review. Retina. 2016;36(12):2250–2264. [PubMed: 27552292]
5. Sadda S, Guymer R, Holz FG, et al. Consensus Definition for Atrophy Associated with Age-Related Macular Degeneration on OCT: Classification of Atrophy Report 3. Ophthalmology. 2018;125(4): 537–548. [PubMed: 29103793]
6. Sayegh RG, Simader C, Scheschy U, et al. A systematic comparison of spectral-domain optical coherence tomography and fundus autofluorescence in patients with geographic atrophy. Ophthalmology. 2011;118(9):1844–1851. [PubMed: 21496928]
7. Zanzottera EC, Ach T, Huisingh C, Messinger JD, Spaide RF, Curcio CA. Visualizing retinal pigment epithelium phenotypes in the transition to geographic atrophy in age-related macular degeneration. Retina (Philadelphia, Pa). 2016;36(Suppl 1):S12–S25.

8. Sarks JP, Sarks SH, Killingworth MC. Evolution of geographic atrophy of the retinal pigment epithelium. Eye (Lond). 1988;2(Pt 5):552–577. [PubMed: 2476333]
9. Li M, Huisingh C, Messinger J, et al. HISTOLOGY OF GEOGRAPHIC ATROPHY SECONDARY TO AGE-RELATED MACULAR DEGENERATION: A Multilayer Approach. Retina. 2018;0:1–7.
10. Smith RT, Koniarek JP, Chan J, Nagasaki T, Sparrow JR, Langton K. Autofluorescence characteristics of normal foveas and reconstruction of foveal autofluorescence from limited data subsets. Invest Ophthalmol Vis Sci. 2005;46(8):2940–2946. [PubMed: 16043869]
11. Xu L, Blonska AM, Pumariega NM, et al. Reticular Macular Disease is Associated with Multilobular Geographic Atrophy in Age-Related Macular Degeneration. Retina. 2013;33(9): 1850–1862. [PubMed: 23632954]
12. Wu Z, Luu CD, Ayton LN, et al. Fundus Autofluorescence Characteristics of Nascent Geographic Atrophy in Age-Related Macular Degeneration. Investigative Ophthalmology & Visual Science. 2015;56(3):1546–1552. [PubMed: 25678689]
13. Wu Z, Luu CD, Ayton LN, et al. Optical Coherence Tomography–Defined Changes Preceding the Development of Drusen-Associated Atrophy in Age-Related Macular Degeneration. Ophthalmology. 2014;121(12):2415–2422. [PubMed: 25109931]
14. Pfau M, Lindner M, Goerdt L, et al. PROGNOSTIC VALUE OF SHAPE-DESCRIPTIVE FACTORS FOR THE PROGRESSION OF GEOGRAPHIC ATROPHY SECONDARY TO AGE-RELATED MACULAR DEGENERATION. RETINA. 2018;0:13.
15. Holz FG, Bindewald-Wittich A, Fleckenstein M, Dreyhaupt J, Scholl HPN, Schmitz-Valckenberg S. Progression of Geographic Atrophy and Impact of Fundus Autofluorescence Patterns in Age-related Macular Degeneration. American Journal of Ophthalmology. 2007;143(3):463–472.e462. [PubMed: 17239336]
16. Bearelly S, Khanifar AA, Lederer DE, et al. Use of fundus autofluorescence images to predict geographic atrophy progression. Retina. 2011;31(1):81–86. [PubMed: 20890245]
17. Maho Oishi AO, Lindner Moritz, Maximillian Pfau, Schmitz-Valckenberg Steffen, Holz Frank G., Monika Fleckenstein. Structural Changes in Optical Coherence Tomography Underlying Spots of Increased Autofluorescence in the Perilesional Zone of Geographic Atrophy. Invest Ophthalmol Vis Sci. 2017;58(7):3303–3310. [PubMed: 28666281]
18. Rudolf M, Vogt SD, Curcio CA, et al. Histologic basis of variations in retinal pigment epithelium autofluorescence in eyes with geographic atrophy. Ophthalmology. 2013;120(4):821–828. [PubMed: 23357621]
19. Agee JM, Ahmad M, Rastogi A, et al. Fundus Autofluorescence Patterns within Geographic Atrophy (GA) in Age-Related Macular Degeneration. Investigative Ophthalmology & Visual Science. 2017;58(8):34–34.
20. Sacconi R, Corbelli E, Carnevali A, Querques L, Bandello F, Querques G. OPTICAL COHERENCE TOMOGRAPHY ANGIOGRAPHY IN GEOGRAPHIC ATROPHY. Retina. 2017;0(0):1–6.
21. Curcio CA, Zanzottera EC, Ach T, Balaratnasingam C, Freund KB. Activated Retinal Pigment Epithelium, an Optical Coherence Tomography Biomarker for Progression in Age-Related Macular Degeneration. Investigative Ophthalmology & Visual Science. 2017;58(6):BIO211–BIO226. [PubMed: 28785769]
22. Fleckenstein M, Charbel Issa P, Helb HM, et al. High-resolution spectral domain-OCT imaging in geographic atrophy associated with age-related macular degeneration. Invest Ophthalmol Vis Sci. 2008;49(9):4137–4144. [PubMed: 18487363]
23. Li M, Huisingh C, Messinger J, et al. HISTOLOGY OF GEOGRAPHIC ATROPHY SECONDARY TO AGE-RELATED MACULAR DEGENERATION: A Multilayer Approach. Retina. 2018;38(10):1937–1953. [PubMed: 29746415]
24. Pfau M, Muller PL, von der Emde L, et al. MESOPIC AND DARK-ADAPTED TWO-COLOR FUNDUS-CONTROLLED PERIMETRY IN GEOGRAPHIC ATROPHY SECONDARY TO AGE-RELATED MACULAR DEGENERATION. Retina. 2018.
25. Schmitz-Valckenberg S, Fleckenstein M, Gobel AP, Hohman TC, Holz FG. Optical coherence tomography and autofluorescence findings in areas with geographic atrophy due to age-related macular degeneration. Invest Ophthalmol Vis Sci. 2011;52(1):1–6. [PubMed: 20688734]

26. Simader C, Sayegh RG, Montuoro A, et al. A longitudinal comparison of spectral-domain optical coherence tomography and fundus autofluorescence in geographic atrophy. American journal of ophthalmology. 2014;158(3):557–566.e551. [PubMed: 24879944]

27. Bearelly S, Chau FY, Koreishi A, Stinnett SS, Izatt JA, Toth CA. Spectral domain optical coherence tomography imaging of geographic atrophy margins. Ophthalmology. 2009;116(9): 1762–1769. [PubMed: 19643488]

28. Wolf-Schnurrbusch UEK, Enzmann V, Brinkmann CK, Wolf S. Morphologic Changes in Patients with Geographic Atrophy Assessed with a Novel Spectral OCT–SLO Combination. Investigative Ophthalmology & Visual Science. 2008;49(7):3095–3099. [PubMed: 18378583]

29. Greferath U, Guymer RH, Vessey KA, Brassington K, Fletcher EL. Correlation of Histologic Features with In Vivo Imaging of Reticular Pseudodrusen. Ophthalmology. 2016;123(6):1320–1331. [PubMed: 27039021]

30. Kim SY, Sadda S, Humayun MS, de Juan E Jr., Melia BM, Green WR. MORPHOMETRIC ANALYSIS OF THE MACULA IN EYES WITH GEOGRAPHIC ATROPHY DUE TO AGE-RELATED MACULAR DEGENERATION. RETINA. 2002;22(4).

31. Smith RT. New Understanding of Age-Related Macular Degeneration Through Quantitative Autofluorescence. JAMA Ophthalmol. 2016;134(7):824–826. [PubMed: 27254789]

32. Greenberg JP, Duncker T, Woods RL, Smith RT, Sparrow JR, Delori FC. Quantitative fundus autofluorescence in healthy eyes. Invest Ophthalmol Vis Sci. 2013;54(8):5684–5693. [PubMed: 23860757]

33. Tan ACS, Pilgrim MG, Fearn S, et al. Calcified nodules in retinal drusen are associated with disease progression in age-related macular degeneration. Science translational medicine. 2018;10(466).

This study uses a precise co-registration method to compare geographic atrophy characteristics on optical coherence tomography and fundus autofluorescence imaging. Photoreceptor layer thickness decreases more significantly than retinal pigment epithelium thickness with decreased autofluorescence levels.

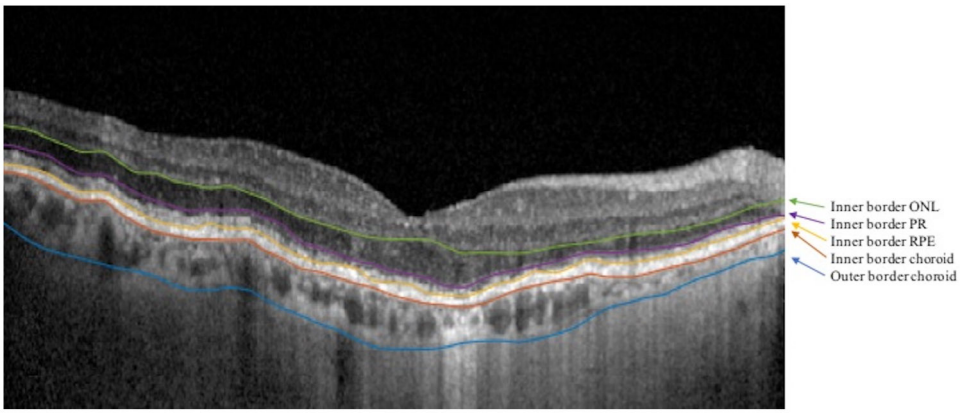

Figure 1: Retinal Layer Segmentations

SD-OCT B-scan image in an eye of a patient with GA. The B-scan shows manually segmented and smoothed borders separating the layers of interest (arrows). For simplicity, the outer border of the outer nuclear layer (ONL) is the inner border of the photoreceptor (PR) layer (purple); the outer border of the PR layer is the inner border of the retinal pigment epithelium (RPE) (yellow), and the outer border of the RPE is the inner border of the choroid (red).

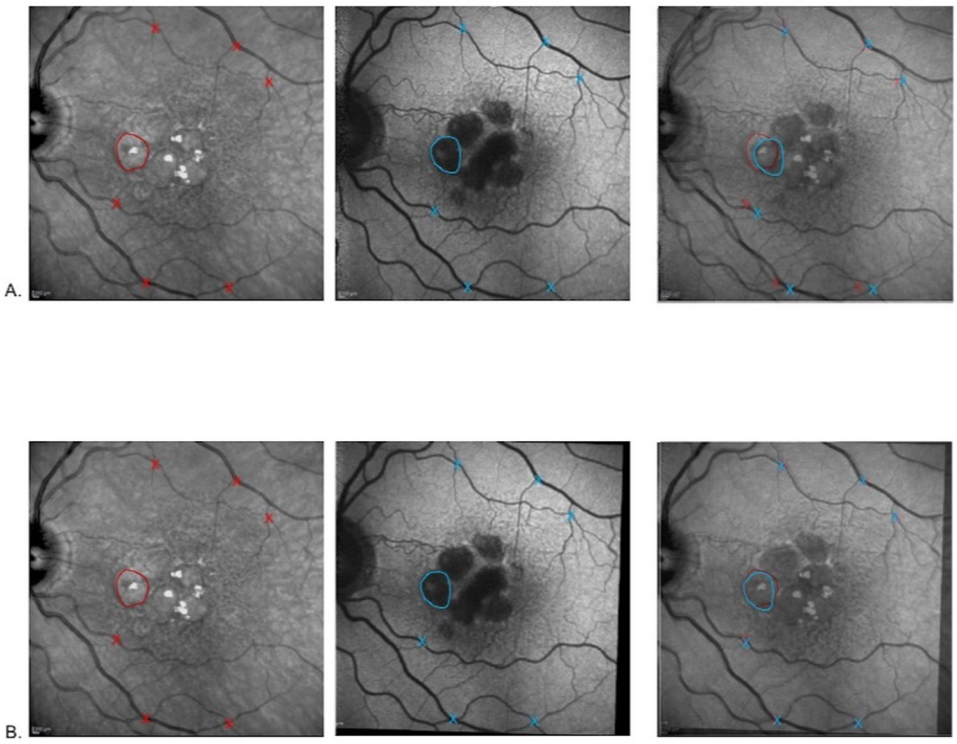

Figure 2: Feature Correspondence by Image registration.

Row A. NIR-R image with a GA lobule outlined in red and vessel crossings, red Xs. Original (not co-registered) FAF image with the same GA lobule outlined in blue and same vessel crossings, blue Xs. With both images overlaid in Photoshop with partial transparency (last panel), there is evident discrepancy between the locations of the same lobule and the vessel crossings. **Row B.** Same sequence as in Row A, but with the FAF image co-registered to the NIR-R image. The handdrawn outlines of the GA lobule and vessel crossings in the last panel nearly coincide.

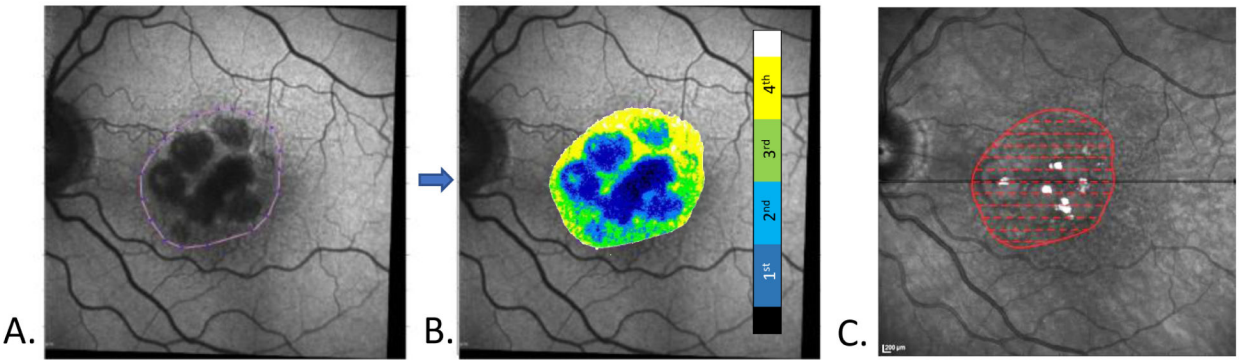

Figure 3: Data extraction from co-registered FAF, NIR-R and SD-OCT scans

A. FAF grayscale image. The border of a manually selected region of interest (ROI) is drawn around the GA lobules. The image itself has been rotated and co-registered with the NIR-R image, **C.** Note the myriad matching SDD in the FAF and NIR-R images, with more seen in the NIR-R image. **B.** The FAF ROI was analyzed and color-coded by dividing the FAF gray levels into quartiles (color bar) after excluding the highest and lowest 2.5% of values (white and black on color bar, respectively). **C.** The AF ROI outline (red) was superimposed onto the co-registered NIR-R image. The SD-OCT scans (not shown) are all automatically registered to the NIR-R image at acquisition. Dashed red lines indicate the locations of the registered B-scan segments from which thickness measurements of the retinal layers and choroid were obtained, and the points from which the FAF quartile values were extracted from **B.**

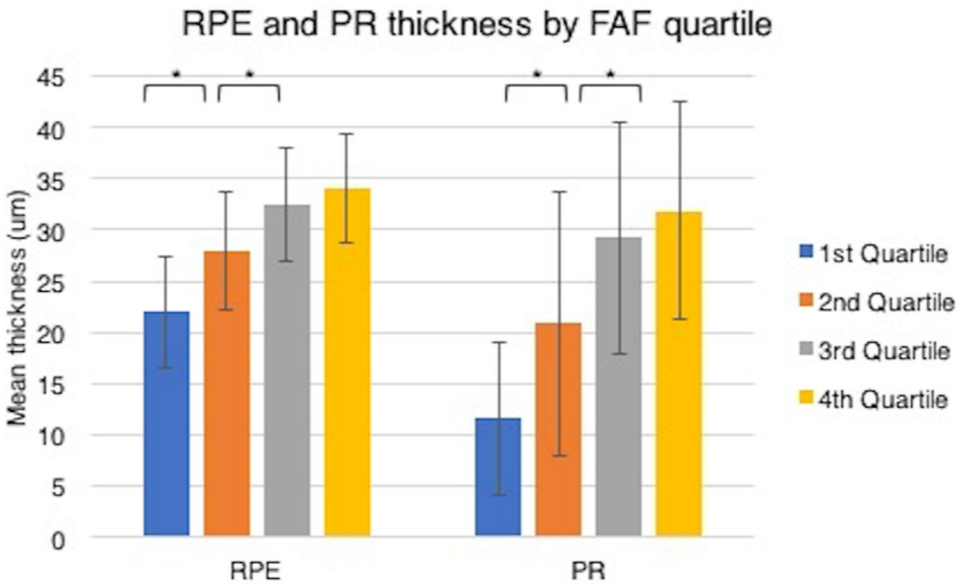

Figure 4: Retinal layer mean thicknesses.

The retinal pigment epithelium (RPE) and photoreceptor layer (PR) mean thicknesses across the FAF quartiles (error bars, SD) were significantly different, specifically between the first, second, and third quartiles (starred brackets) by *post hoc* analysis (Tukey multiple comparison test, $p < 0.01$).

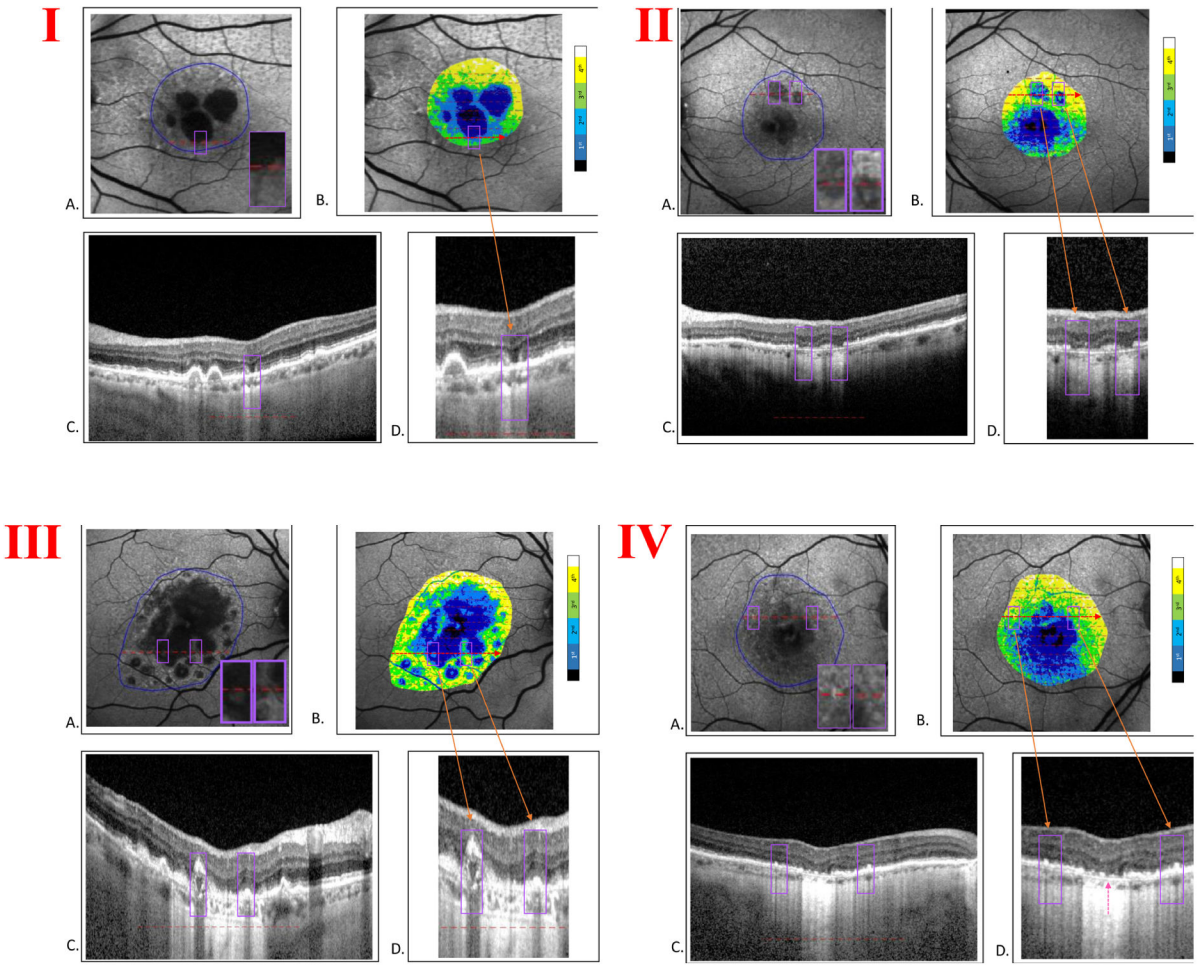

Figure 5: Correlation of FAF quartiles with SD-OCT features and stages of atrophy.

In each large panel (**I, II, III, IV**) there are four images: **A.** FAF image of geographic atrophy (GA) with region of interest (ROI) outlined (solid blue line). Inset, violet box(es) shows zoomed-in detail of feature(s) of interest. **B.** ROI color-coded by adjacent scale bar after dividing FAF gray levels into quartiles, superimposed on FAF grayscale image. The violet box(es) include the same area(s) as in **A. C.** SD-OCT B-scan segment at level of red dashed line in **A**. Here the violet box delimits the *linear horizontal* extent of the B-scan that passes through the *two-dimensional* violet box in **A** along the red line. **D.** Zoomed-in view of the B-scan segment in **C**. The violet box(es), orange arrow(s), include the B-scan segment through the same feature(s) of interest.

Panel I. A. FAF image with feature of interest, GA transition zone (violet box) **B.** ROI color-coded by FAF quartiles. **C.** B-scan segment through the ROI in **A** along the red line. **D.** Zoomed-in view of the B-scan segment in C. The violet box (orange arrow) includes on each side the border between the central hypoautofluorescent GA and relatively preserved transition zones with some discontinuous hypertransmission and irregular EZ (incomplete RPE and outer retinal atrophy, iRORA). The B-scan demonstrates sharp ELM descent on each side of the GA lobule, in which FAF is in the first quartile but hypertransmission is still

discontinuous, consistent with residual RPE, while the PR layer is completely collapsed, constituting complete outer retinal atrophy, cORA, but not cRORA.

Panel II. A. FAF image with features of interest, two GA lobules with non-uniform FAF, insets (violet boxes). Red dashed line, location of B-scan segment in **C**. **B.** ROI color-coded by FAF quartiles. The non-uniform GA lobules include a mixture of quartiles. **C.** B-scan segment through GA lobules. **D.** Zoomed-in view of the B-scan through the features of interest (violet boxes), the GA lobules with non-uniform FAF (orange arrows), with increased choroidal reflectivity, demonstrating partial RPE as well as PR dropout, or iRORA.

Panel III. A. FAF image with zoomed-in details of features of interest (violet boxes), areas of relatively preserved FAF within/between larger GA lobules. Red dashed line indicates location of the B-scan in **C**. **B.** ROI color-coded by FAF quartiles. The preserved areas of FAF (violet boxes) fall in quartiles 2 and 3. **C.** B-scan segment through features of interest in **A**. There appear to be at least two structures (yellow arrows) displaying heterogeneous internal reflectivity within drusen (HIRD), which have been identified as hydroxyapatite nodules and may be indicators of progression to advanced AMD.[33] **D.** Zoomed-in view of the B-scan through areas of quartiles 2/3 FAF demonstrates preserved islands of migrating and heaped up RPE, respectively, that show strikingly normal choroidal reflectivity. The outer retina is absent in the first, thus meeting the definition of complete outer retinal atrophy (cORA), and disorganized but not absent in the second, thus meeting the definition of incomplete outer retinal atrophy (iORA).

Panel IV. A. FAF image shows zoomed-in details of features of interest (violet boxes), reticular autofluorescence near the GA lobules. Red dashed line indicates the location of the B-scan in **C**. **B.** ROI color-coded by FAF quartiles. **C.** B-scan segment through the features of interest (violet boxes), reticular autofluorescence. **D.** Zoomed-in view of the B-scan that crosses through the reticular FAF patterns, which fall in FAF quartiles 3 and 4 in **B,** as well as through an early GA lobule in the center, which falls in FAF quartiles 1 and 2. The B-scan through the reticular AF demonstrates multiple subretinal drusenoid deposits (SDD), orange arrows. The RPE is irregular throughout and appears to be lifting off Bruch's membrane temporally. The early GA lobule shows partially preserved AF, mixed quartiles 1 and 2, with remaining RPE segments, but the outer retina is obliterated (magenta arrow), resulting in complete outer retinal atrophy (cORA).

Table 1:
Thickness (um) of outer retinal layers across FAF quartiles

Mean thicknesses and standard deviations (SD) of the four layers (choroid, RPE, PR, and ONL) across all eyes in each of the FAF quartiles. p-values are for overall ANOVA with repeated measures with a within-subjects factor.

Layer	choroid				RPE				PR				ONL			
Quartile	**1st**	**2nd**	**3rd**	**4th**	**1st**	**2nd**	**3rd**	**4th**	**1st**	**2nd**	**3rd**	**4th**	**1st**	**2nd**	**3rd**	**4th**
Mean (SD)	154.5 (47.7)	157.0 (45.9)	161.0 (43.7)	162.8 (43.9)	22.0* (5.4)	27.9* (5.7)	32.46* (5.5)	34.0 (5.3)	11.6* (7.4)	20.9* (12.9)	29.2* (11.3)	32.2 (10.7)	37.2 (15.5)	43.8 (17.8)	48.6 (13.8)	47.8 (11.8)
p-value	0.94				**<0.001**				**<0.001**				0.015			